RESEARCH PAPER

The saponin D39 blocks dissociation of non-muscular myosin heavy chain IIA from TNF receptor 2, suppressing tissue factor expression and venous thrombosis

Correspondence Dr Boyang Yu and Dr Junping Kou, State Key Laboratory of Natural Products, Jiangsu Key Laboratory of TCM Evaluation and Translational Research, Department of Complex Prescription of TCM, China Pharmaceutical University, 639 Longmian Road, Nanjing 211198, China. E-mail: boyangyu59@163.com; junpingkou@cpu.edu.cn

Ke-feng Zhai[1,2] iD, Jin-rong Zheng[1], You-mei Tang[1], Fang Li[1], Yan-ni Lv[1], Yuan-yuan Zhang[1], Zhen Gao[3], Jin Qi[1], Bo-yang Yu[1] and Jun-ping Kou[1]

[1]State Key Laboratory of Natural Products, Jiangsu Key Laboratory of TCM Evaluation and Translational Research, Department of Complex Prescription of TCM, China Pharmaceutical University, Nanjing, China, [2]Institute of Pharmaceutical Biotechnology, School of Biological and Food Engineering, Suzhou University, Suzhou, China, and [3]Department of Medicine-Ather&Lipo, Baylor Colledge of Medicine, Houston, TX, USA

BACKGROUND AND PURPOSE
Non-muscular myosin heavy chain IIA (NMMHC IIA) plays a key role in tissue factor expression and venous thrombosis. Natural products might inhibit thrombosis through effects on NMMHC IIA. Here, we have shown that a natural saponin, D39, from *Liriope muscari* exerted anti-thrombotic activity *in vivo*, by targeting NMMHC IIA.

EXPERIMENTAL APPROACH
Expression and activity of tissue factor in endothelial cells were analysed *in vitro* by Western blot and simplified chromogenic assays. Interactions between D39 and NMMHC IIA were assessed by serial affinity chromatography and molecular docking analysis. D39-dependent interactions between NMMHC IIA and TNF receptor 2 (TNFR2) were measured by immunofluorescence, co-immunoprecipitation and proximity ligation assays. Anti-thrombotic activity of D39 *in vivo* was evaluated with a model of inferior vena cava ligation injury in mice.

KEY RESULTS
D39 inhibited tissue factor expression and procoagulant activities in HUVECs and decreased thrombus weight in inferior vena cava-ligated mice dose-dependently. Serial affinity chromatography and molecular docking analysis suggested that D39 bound to NMMHC IIA. In HEK293T cells, D39 inhibited tissue factor expression evoked by NMMHC IIA overexpression. This effect was blocked by NMMHC IIA knockdown in HUVECs. D39 inhibited dissociation of NMMHC IIA from TNFR2, which subsequently modulated the Akt/GSK3β–NF-κB signalling pathways.

CONCLUSIONS AND IMPLICATIONS
D39 inhibited tissue factor expression and thrombus formation by modulating the Akt/GSK3β and NF-κB signalling pathways through NMMHC IIA. We identified a new natural product that targeted NMMHC IIA, as a potential treatment for thrombotic disorders and other vasculopathies.

Abbreviations
DVT, deep vein thrombosis; D39, saponin D39; IVCL, inferior vena cava ligation; NMMHC IIA, non-muscle myosin heavy chain IIA; PLA, proximity ligation assays; TF, tissue factor; TNFR2, tumour necrosis factor receptor II.

Tables of Links

TARGETS	
Catalytic receptors[a]	PI3K
TNFR2	MRLC
Enzymes[b]	**Other protein targets**[c]
Akt	Factor Xa
GSK3β	

LIGANDS	
TNF-α	Wortmannin
CHIR99021	

These Tables list key protein targets and ligands in this article that are hyperlinked to corresponding entries in http://www.guidetopharmacology.org, the common portal for data from the IUPHAR/BPS Guide to PHARMACOLOGY (Southan *et al.*, 2016), and are permanently archived in the Concise Guide to PHARMACOLOGY 2015/16 ([a,b,c]Alexander *et al.*, 2015a,b,c).

Introduction

Deep vein thrombosis (DVT) is a common condition that is characterized by the formation of an occlusive blood clot in the venous vascular system, which occurs most often in the large veins of the legs (Schulz *et al.*, 2013). DVT and its various adverse outcomes, including pulmonary embolism, are the third leading cause of cardiovascular-associated death after myocardial infarction and stroke (Mackman, 2008; Mackman, 2012). Tissue factor (TF) is a key trigger of blood coagulation and an important determinant of the hypercoagulable state that is associated with venous thrombosis (Li *et al.*, 2009; Mackman, 2012). Inhibition of TF may represent an effective strategy for DVT treatment (Mackman, 2012; Zhai *et al.*, 2015).

Non-muscle myosin II is an actin-based motor protein that is essential for a variety of physiological and pathological functions (Liu *et al.*, 2010; Maravillas-Montero and Santos-Argumedo, 2012; Lv *et al.*, 2013; Badirou *et al.*, 2015). Non-muscle myosin heavy chain IIA (NMMHC IIA) is one of the isoforms of non-muscle myosin II, and earlier studies have suggested that its deficiency or inhibition can reduce platelet aggregation, TF expression and arterial thrombus formation (Calaminus *et al.*, 2007; Leon *et al.*, 2007; Ono *et al.*, 2008). Our recent study has shown that NMMHC IIA inhibition or knockdown decreases TF expression and DVT mainly through the Akt/GSK3β-NF-κB signalling pathway. NMMHC IIA inhibition or stabilization of the NMMHC IIA-TNF receptor II (TNFR2) interaction is a novel potential strategy for the treatment of venous thrombosis and other inflammation-related thrombotic diseases (Zhai *et al.*, 2015).

Natural products, as used in traditional Chinese medicine, are a major resource for drug discovery as they include a wide variety of chemicals with structural diversity and novel molecular scaffolds. *Ophiopogon japonicus* and *Liriope muscari* are two traditional Chinese herbs that have been widely used throughout history in China to treat acute and chronic inflammatory diseases, as well as cardiovascular diseases. Recent evidence suggests that saponins, including ruscogenin, ophiopogonin D and DT-13, found in extracts of these two herbs are involved in anti-inflammatory and anti-thrombotic activity, as well as inhibition of TF (Liu *et al.*, 2002; Kou *et al.*, 2006; Huang *et al.*, 2008; Sun *et al.*,

2010; Sun *et al.*, 2012; Tian *et al.*, 2013). Furthermore, our previous study indicated that saponin compounds are potential NMMHC IIA inhibitors, based on NMMHC IIA homology modelling and virtual screening (Lv *et al.*, 2013). In addition, we have used molecular docking and an *in vitro* assay to comprehensively evaluate the effects of 16 ophiopogon saponin derivatives that were isolated from *L. muscari*, on NMMHC IIA binding energy and TF expression. The results revealed that eight compounds showed good binding affinity to NMMHC IIA and markedly down-regulated TF protein expression. Among them, D39 (whose chemical structure is shown in Figure 1A) showed the lowest binding energy for NMMHC IIA and significantly down-regulated TF expression (Supporting Information Figure S1). In the present study, we have investigated the effects and underlying mechanisms of D39 on NMMHC IIA-dependent TF expression and DVT. Our studies showed that D39 down-regulated endothelial TF expression and venous thrombus formation by modulating the PI3K/Akt/GSK3β and NF-κB signalling pathways. Molecular docking analysis and serial affinity chromatography indicated the possible binding of D39 to NMMHC IIA, which was confirmed by the gain-of-function and loss-of-function studies of NMMHC IIA in HEK293T cells and HUVECs. In addition, D39 inhibited the dissociation of NMMHC IIA from TNFR2 both *in vitro* and *in vivo*. These findings suggested that NMMHC IIA mediated the anti-thrombotic activity of D39 and that D39 could be a potential therapy for DVT and other vasculopathies.

Methods

Cell culture

HUVECs, primary HUVECs, EA.hy 926 endothelial cells and HEK 293T cells were maintained at 37°C in a humidified incubator with 5% CO_2 and were cultured in growth medium (DMEM). EA.hy 926 endothelial cells and HEK 293T were from American Type Culture Collection (Manassas, VA, USA). HUVECs and primary HUVECs (Lot Number 5138) were from Sciencell Research Laboratories, Inc. (Carlsbad, CA, USA). The companies have ethical permission for work with human tissue and the patients' permissions to use the cells.
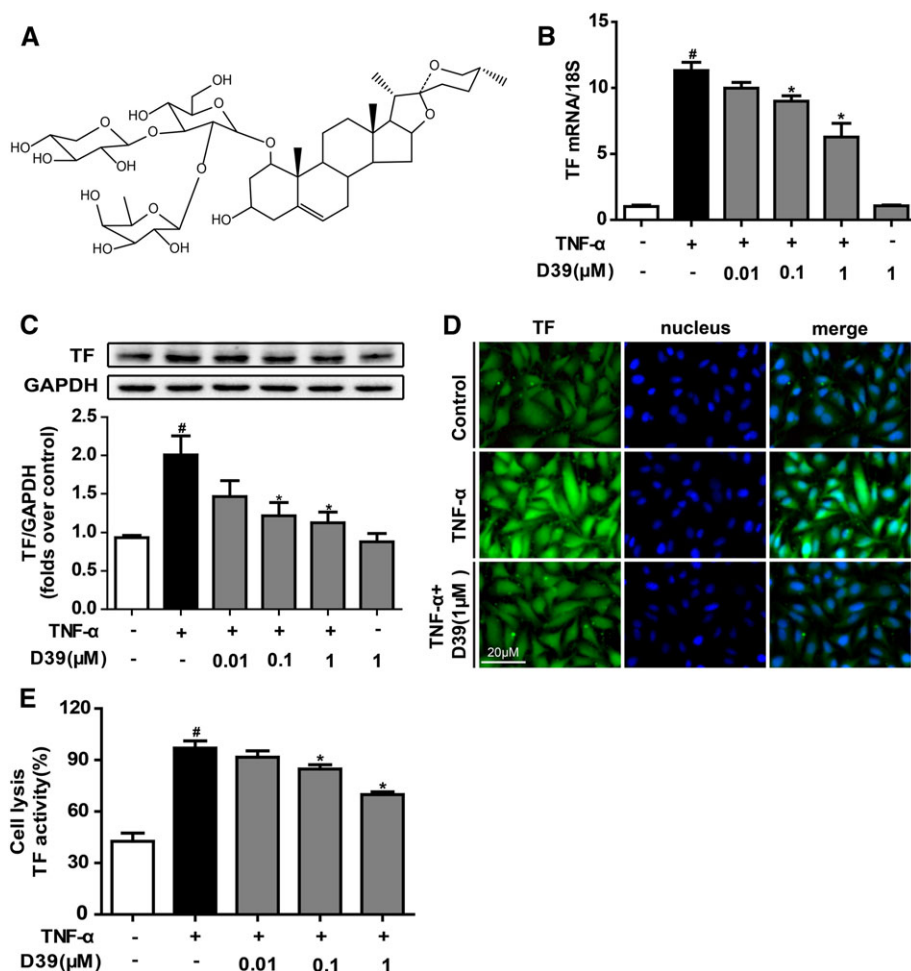
A

B

C

D

E

Figure 1

D39 suppressed TNF-α-induced TF expression and procoagulant activity in HUVECs. HUVECs were pretreated with D39 for 1 h at various concentrations followed by TNF-α (10 ng·mL^{-1}) stimulation for 5 h. (A) The structure of saponin D39. (B) TF mRNA expression levels after TNF-α exposure, with or without D39 (0.01–1 μM). (C, D) TF protein expression was analysed by Western blots and immunofluorescence. (E) TF procoagulant activities in cell lysates were examined with a chromogenic assay. Data shown are the means ± SEM of five independent experiments. [#]$P < 0.05$, significantly different from the unstimulated group; *$P < 0.05$, significantly different from the TNF-α-stimulated group.

Western blot analysis

Cell lysates were prepared, and protein concentrations were determined by the bicinchoninic acid protein assay. Equivalent amounts of total proteins were separated by 10% SDS-PAGE, subjected to immunoblotting, probed with the respective antibodies and detected using HRP-conjugated secondary antibodies coupled with ECL.

Molecular docking

All ligands were constructed in Sybyl x1.1 and then applied to all hydrogen and Gastiger–Huckel charges in Sybyl in the Tripos force field under an implicit solvent environment. The minimization steps included 1000 cycles of the steepest descent until the convergent threshold of 0.05 kcal^{-1}·Å^{-1} was satisfied. All ligands were docked into the binding site of a homology model of NMMHC IIA (Lv *et al.*, 2013) via GOLD 3.0.1. The centre of the grid was placed at the centre of the receptor binding site, with grid dimensions of (15, 15,

and 15 Å). Ten conformers were generated from random configurations of the ligand with fully flexible torsion degrees of freedom. The GoldScore function of GOLD 3.0.1 was employed to estimate the binding energies (Trott and Olson, 2010). The indices were chosen as twice the speed calculation, while Van der Waals forces and hydrogen bonding parameters were set to 6.0 and 3.0 respectively. The highest score ranked by GoldScore and ChemScore was chosen for further research (Banerji *et al.*, 2007).

Simplified chromogenic assay

The cell lysates were frozen and thawed three times before they were used in the assay. The cell surfaces were washed three times by PBS. Mouse plasma was prepared by centrifugation at 3000× *g* for 10 min and stored at −70°C before use. TF activity was determined by a chromogenic assay as previously reported (Sun *et al.*, 2012). Samples (45 μL) were incubated with Tris-CaCl$_2$ buffer (5 μL, pH 7.3) containing human prothrombin complex in a 96-well plate and

incubated at 37°C for 30 min. Then, 50 µL of Tris-EDTA buffer (pH 8.4) containing chromogenic substrate Xa was added to each well. The absorbance was measured at 405 nm. The TF activity of the control group was taken as 100%.

Immunofluorescence analysis

After the experimental period, HUVECs and primary HUVECs were fixed with 4% paraformaldehyde for 30 min, permeabilized with 0.1% Triton X-100 solution for 30 min and blocked with BSA (5 mg·mL^{-1} in PBS) for 1 h. Cells were incubated with primary antibodies overnight at 4°C, washed three times with PBS, incubated with Alexa Fluor 488-/594-labelled secondary antibody in PBS for 1 h, incubated in DAPI solution for 5 min and then analysed using a fluorescence microscope (Leica, Mannheim, Germany) or a laser confocal microscope (Leica, Mannheim, Germany).

Real-time qRT-PCR

Total RNA was extracted using TRIzol (Invitrogen, Carlsbad, CA, USA) following the manufacturer's instructions. First-strand cDNA was synthesized from total RNA using a first-strand cDNA synthesis kit (Vazyme Biotech, Nanjing, Jiangsu, China) according the manufacturer's recommendations. Real-time quantitative PCR was performed in a 96-well plate using SYBR Green Master Mix (Bio-Rad, Hercules, CA, USA). The following forward and reverse primers were used for amplification: hTF forward, GAACCCAAACCCGTCAAT; hTF reverse, TCTCATACAGAGGCTCCC; h18S forward, AAACGGCTACCACATCCAAG and h18S reverse, CCTCCA ATGGATCCTCGTTA. The reaction was conducted with an initial denaturing step at 95°C for 5 min and then underwent 40 cycles of 95°C for 10 s and 60°C for 30 s. Relative gene expression data were analysed using the $2^{-\Delta\Delta Ct}$ method.

Serial affinity chromatography

Separation and identification of target proteins using serial affinity chromatography was performed as described previously with some modifications (Yamamoto et al., 2006; Ju et al., 2012). Briefly, lysate from endothelial cells (1.0 mL) was stirred gently with the D39 affinity resin (30 µL) (Epoxy activated-Sepharose™ 6B, EAS6B, GE Healthcare) at 4°C for approximately 1.5 h and was then precipitated by centrifugation at 16 000 × g for 1 min. The resulting supernatant was mixed with another 30 µL of the D39 affinity resin at 4°C, again for approximately 1.5 h. The resulting resin was washed three times with 1.0 mL of lysate buffer, resuspended in 30 µL of 2 × loading buffer, heated in boiling water for 5 min and then centrifuged for 1 min. The supernatant was subjected to SDS-PAGE. The resulting bands were stained with silver staining and then comparatively analysed to identify specific binding proteins. For reproducibility, the above procedures were carried out 3-5 times.

Human NMMHC IIA knockdown

As described in our previous report (Zhai et al., 2015), the sequences of the siRNAs used to suppress NMMHC IIA expression were 5-GAGGCAAUGAUCACUGACUdTdT-3 and 5-AGUCAGUGAUCAUUGCCUCdTdT-3, and they were designed and synthesized by Biomics Biotechnologies Co., Ltd. (Nantong, Jiangsu, China). Endothelial cells were seeded in 60 mm dishes and grown to 70–80% confluence, and then

they were transfected with siRNA using ExFect Transfection Reagent. Final concentrations of siRNA or non-silencing siRNA were 100 nM.

Human NMMHC IIA overexpression

The recombinant plasmid pEGFP-NMMHC IIA (EX-T1335-M98) was constructed by the directed cloning technique according to FulenGen (Guangzhou, China). For plasmid transfection, HEK 293T cells were plated on 6-well plates at a density of 4×10^5 cells per well. Transfection of HEK 293T cells was performed using the Endofectin Transfection Reagent (FulenGen, Guangzhou, China) according to the manufacturer's instructions. Briefly, 3 µg of purified pEGFP-NMMHC IIA diluted in 200 µL of Opti-MEM medium was mixed with 9 µg of Endofectin Transfection Reagent that was diluted in 200 µL of Opti-MEM medium. The DNA-Endofectin mixture was incubated for 20 min at room temperature and then added to the 6-well plates. Four hours later, the medium was changed to complete medium. Control cells were mock-transfected with empty vectors as a negative control (Zhai et al., 2015).

Co-immunoprecipitation

The primary HUVECs were lysed in RIPA lysis buffer (25 mM Tris•HCl pH 7.6, 150 mM NaCl, 1% NP-40, 1% sodium deoxycholate and 0.1% SDS) containing protease inhibitor (aprotinin, bestatin, E-64, leupeptin, sodium, orthovanadate, sodium pyrophosphate and β-glycerophosphate). Anti-NMMHC IIA and TNFR2 antibody (Abcam, CA, USA) together with protein A/G agarose were used to immunoprecipitate TNFR2 and NMMHC IIA, respectively, as well as associated proteins. Proteins were resolved by SDS-PAGE and detected by Western blot analysis.

Proximity ligation assays (PLA)

To demonstrate a complex between native TNFR2 and NMMHC IIA in primary HUVECs, a PLA kit (Sigma-Aldrich, St Louis, USA) was used according to the manufacturer's protocols (Soderberg et al., 2008). Primary antibodies against TNFR2 and NMMHC IIA were used, and secondary antibodies were conjugated to oligonucleotides for ligation and subsequent rolling-circle amplification.

Animals

All animal care and experimental procedures were carried out according to the current European Communities Council-ECC guidelines for the care of laboratory animals and ethical guidelines for investigations of experimental pain in conscious animals. In addition, Ethical approval was granted by the Animal Welfare and Ethics Review Board of the University of Bristol, UK. Animal studies are reported in compliance with the ARRIVE guidelines (Kilkenny et al., 2010; McGrath & Lilley, 2015).

Male C57BL/6J mice (20–25 g; 8 weeks; specified pathogen free) were provided by the Model Animal Research Centre of Yangzhou University (Yangzhou, Jiangsu, China) and kept in cages containing standard bedding, with at least five mice per cage. Mice were housed in a specific pathogen-free facility with 12 h light/dark cycle [07 to 19 h, temperature (22 ± 2°C), humidity (40–70%), controlled ventilation] and with sterile water and irradiated food available ad libitum. Animals were

allowed to acclimatize to their housing environment for at least 7 days prior to experimentation and to the experimental room for 1 h before experiments.

Mouse models of deep vein thrombosis

The mice were randomly divided into five groups: sham, those with inferior vena cava ligation (IVCL), IVCL + 0.1 mg·kg^{-1} D39, IVCL + 0.3 mg·kg^{-1} D39 and IVCL + 1 mg·kg^{-1} D39. The mice were injected with vehicle (5% ethanol in saline) or D39 (0.1, 0.3 or 1 mg·kg^{-1}) i.p. and then underwent IVCL to initiate thrombus formation 1 h later.

Before surgery, mice were anaesthetized with ketamine and xylazine (80 mg·kg^{-1} and 10 mg·kg^{-1}, respectively, i.p.) and a midline laparotomy was performed (Singh *et al.,* 2002; Zhai *et al.,* 2015). The small bowel was exteriorized and placed onto a moistened gauze pad next to the animal. The infrarenal IVC was identified, and all side branches were ligated with nonreactive 6-0 Prolene suture. Posterior venous branches were cauterized. A 6-0 Prolene suture was tied down on the IVC, caudally to the left renal vein. After surgery, peritoneum and skin were closed by monofilament suture with asepsis. The animal allowed to recover with good postoperative care, according to the current European Communities Council ECC guidelines for the care of laboratory animals and ethical guidelines for investigations of experimental pain in conscious animals. The post-operative death rate was about 15%. The mice were killed 48 h after IVCL and plasma and the IVC were collected for analysis. The experiment was performed in a blinded manner.

Histology and immunohistochemistry

The excised vessel was dehydrated with 40% sucrose, embedded in optimal cutting temperature (OCT) and frozen at −70°C. The IVC was sectioned into slices of 10 μm of thickness with a cryotome (Leica, Mannheim, Germany). Specimens were washed in PBS and stained with haematoxylin and eosin (H&E). For immunohistochemical staining, slides were incubated with primary antibodies at 4°C overnight. Alexa Fluor 488-/594-labelled antibodies were used as secondary antibodies. The nuclei were stained with DAPI. Pathological changes in IVC were observed under a fluorescence microscope (Leica, Mannheim, Germany).

Data and statistical analysis

The data and statistical analysis in this study comply with the recommendations on experimental design and analysis in pharmacology (Curtis *et al.,* 2015). Results are reported as the mean ± SEM. The data were analysed by two-tailed Student's *t*-test or one-way ANOVA followed by Dunnett *post hoc* tests. A *P* value < 0.05 was considered statistically significant. Data analysis was conducted in blinded manner (single-blind study design).

Materials

The saponins ruscogenin, ophiopogonin D, DT-13, D39, D5, D23, D26, D36, D21, D29, D31, D32, D41, D28, D34-22 and D34-27 (purity > 95%) were extracted and purified from extracts of the root tuber of *L. muscari* by the authors. Stock solutions (50 μM) were made in DMSO and stored at −20°C. FBS was purchased from Invitrogen (Grand Island, NY, USA). DMEM was from GIBCO/BRL (Life Technologies, CA,

USA). Prothrombin complex was from the Hualan Bioengineering Company (Xinxiang, Henan, China). Factor Xa chromogenic substrate, human TNF-α and blebbistatin were purchased from Sigma-Aldrich (St. Louis, MO, USA). CHIR99021 was purchased from Selleckchem (Houston, TX, USA). Antibodies against human tissue factor and mouse tissue factor (for Western blots) were purchased from R&D Systems (Minneapolis, MN, USA). Antibodies against tissue factor (for immunohistochemistry) were purchased from Epitomics (Burlingame, CA, USA). The antibody against GAPDH was from KangChen Bio-tech (Shanghai, China). Antibodies against myosin IIA, p65, phospho-p65, IκBα, phospho-IκBα, Akt, phospho-Akt, GSK3β and phospho-GSK3β were obtained from Cell Signaling Technology (Boston, MA, USA). Wortmannin and DAPI were from Beyotime Biotechnology (Shanghai, China). Antibodies against PI3K and phospho-PI3K as well as HRP-conjugated secondary antibodies were from Bioworld Technology (Minnesota, MN, USA). RIPA lysis buffer, protease inhibitor, a first-strand cDNA synthesis kit, ExFectin transfection reagent and enhanced chemiluminescene (ECL) reagent were from Vazyme Biotech (Nanjing, Jiangsu, China). SYBR Green Master Mix was from Bio-Rad (Hercules, CA, USA). Donkey anti-rabbit IgG (H + L) secondary antibody, donkey anti-goat IgG (H + L) secondary antibody and TRIzol reagent were from Invitrogen (Carlsbad, CA, USA), and all other reagents used in this study were of the highest purity commercially available.

Results

D39 significantly down-regulated TF expression and inhibited procoagulant activity in HUVECs

To further confirm the effects of D39 on TF expression and activity in endothelial cells, the cells were pretreated with D39 (0.01, 0.1 or 1 μM) to suppress TF mRNA and to down-regulate its expression, which is triggered by TNF-α (10 ng·mL^{-1}) in HUVECs in a dose-dependent manner (Figure 1B, C). Immunocytochemistry analysis also confirmed that D39 treatment down-regulated TF expression in HUVECs that were stimulated with TNF-α (Figure 1D). Similarly, D39 inhibited the procoagulant activity of TF, as determined by a simplified chromogenic assay (Figure 1E).

D39 activated the Akt/GSK3β signalling pathway and inhibited NF-κB p65 nuclear translocation in HUVECs

The PI3K/Akt signalling pathway negatively regulates TF expression *in vitro* and *in vivo*. In our present experiments, D39 pretreatment significantly up-regulated phospho-PI3K, phospho-Akt and phospho-GSK3β in TNF-α-treated cells (Figure 2A–C). To further determine whether TF expression is also modulated by the PI3K/Akt/GSK3β signalling pathway in endothelial cells, we examined TNF-α-induced TF expression in the presence of the PI3K inhibitor wortmannin or the GSK3β inhibitor CHIR99021. The results showed that wortmannin blocked the inhibitory action of D39 (Supporting Information Figure S3B) and CHIR99021 enhanced the inhibitory effects of D39 on TF
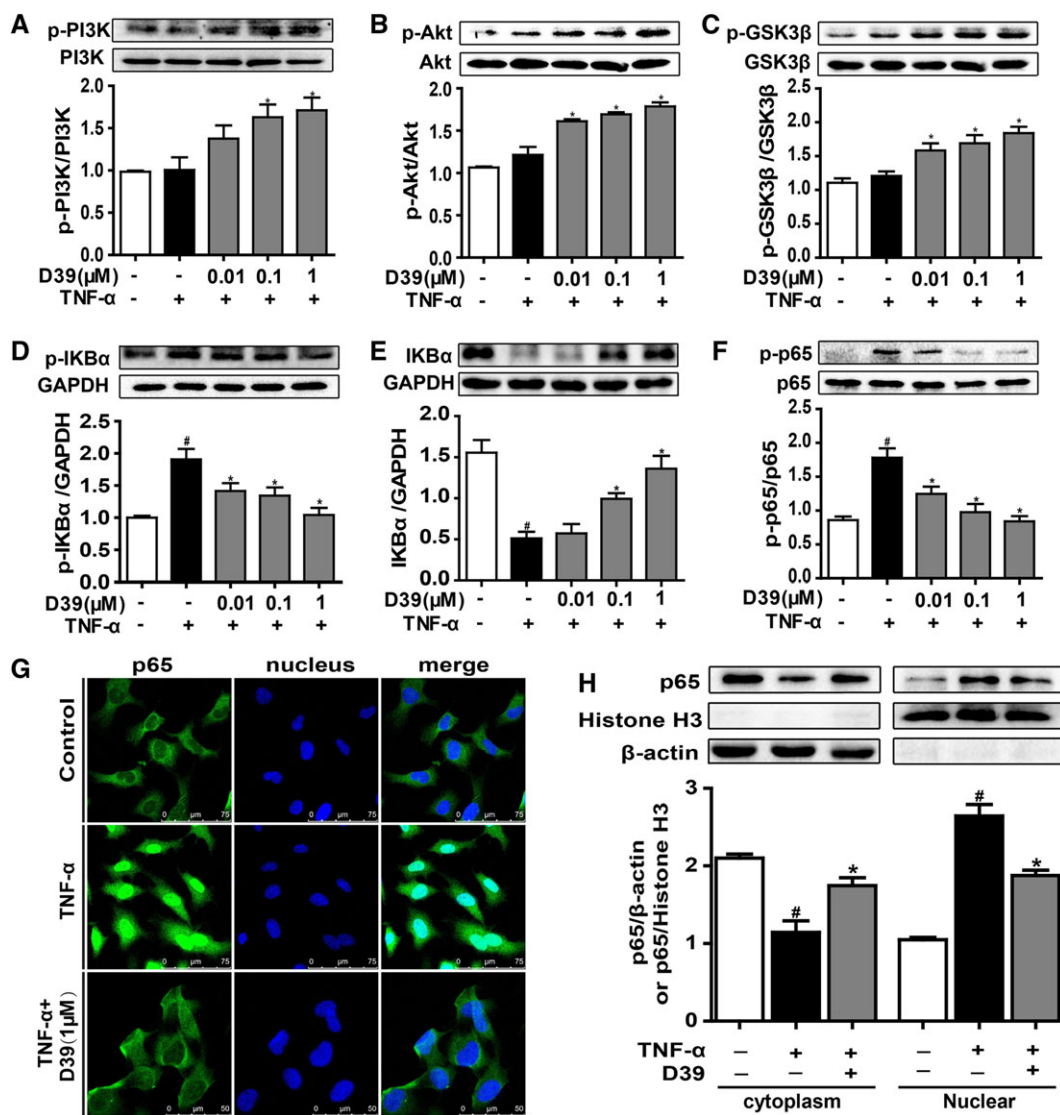
Figure 2

D39 activated the PI3K/Akt signalling pathway and inhibited NF-κB p65 nuclear translocation in endothelial cells. HUVECs and primary HUVECs were treated with TNF-α (10 ng·mL^{-1}) and D39 (1 μM) for different durations and lysed. (A–C) PI3K, Akt and GSK3β as well as phosphorylated PI3K, Akt and GSK3β were assessed by Western blots. (D–F) IκBα and p65 as well as phosphorylated IκBα and p65 were assessed by Western blots. (G) Immunofluorescence staining of NF-κB p65 in primary HUVECs after treatment with 1 μM D39 for 1 h followed by 30 min stimulation with TNF-α (10 ng·mL^{-1}) or vehicle. Scale bar, 50 μm. (H) NF-κB p65 protein expression in the cytoplasm and nucleus of D39-treated primary HUVECs. Cells were pretreated with 1 μM D39 for 1 h and stimulated with TNF-α (10 ng·mL^{-1}) for 30 min. Proteins were extracted from the cytoplasm and nucleus, using β-actin and histone H3 as the internal standards. Data shown are the means ± SEM ($n = 5$ in five individual experiments) for the cell line experiments. $^{\#}P < 0.05$, significantly different from the unstimulated group; $^{*}P < 0.05$, significantly different from the TNF-α-stimulated group.

expression (Supporting Information Figure S3A), indicating that D39 reduced TF expression through PI3K/Akt signalling by suppressing GSK3β activity.

NF-κB/p65 is a transcription factor that regulates TF expression. Inactivated GSK 3β (p-GSK 3β) prevents degradation of IκBα and p65 nuclear translocation (Guha and Mackman, 2002; Zhang *et al.*, 2010). As shown in Figure 2D, E, TNF-α induced IκBα phosphorylation and IκBα degradation, but these effects were inhibited by D39. TNF-α-induced NF-κB p65 phosphorylation was also attenuated by D39 (Figure 2F). D39 abolished the TNF-α-

induced nuclear localization of p65 in primary HUVECs, and its expression was similar to that in controls (Figure 2G, H). This suggested a key role for D39 in down-regulating TF expression via the NF-κB pathway (Figure 2G, H).

NMMHC IIA mediated the inhibitory effects of D39 on TF expression

Using the D39 affinity medium, we captured specific binding proteins for D39 from HUVEC lysates by serial affinity chromatography, as illustrated in Figure 3A. The amount of
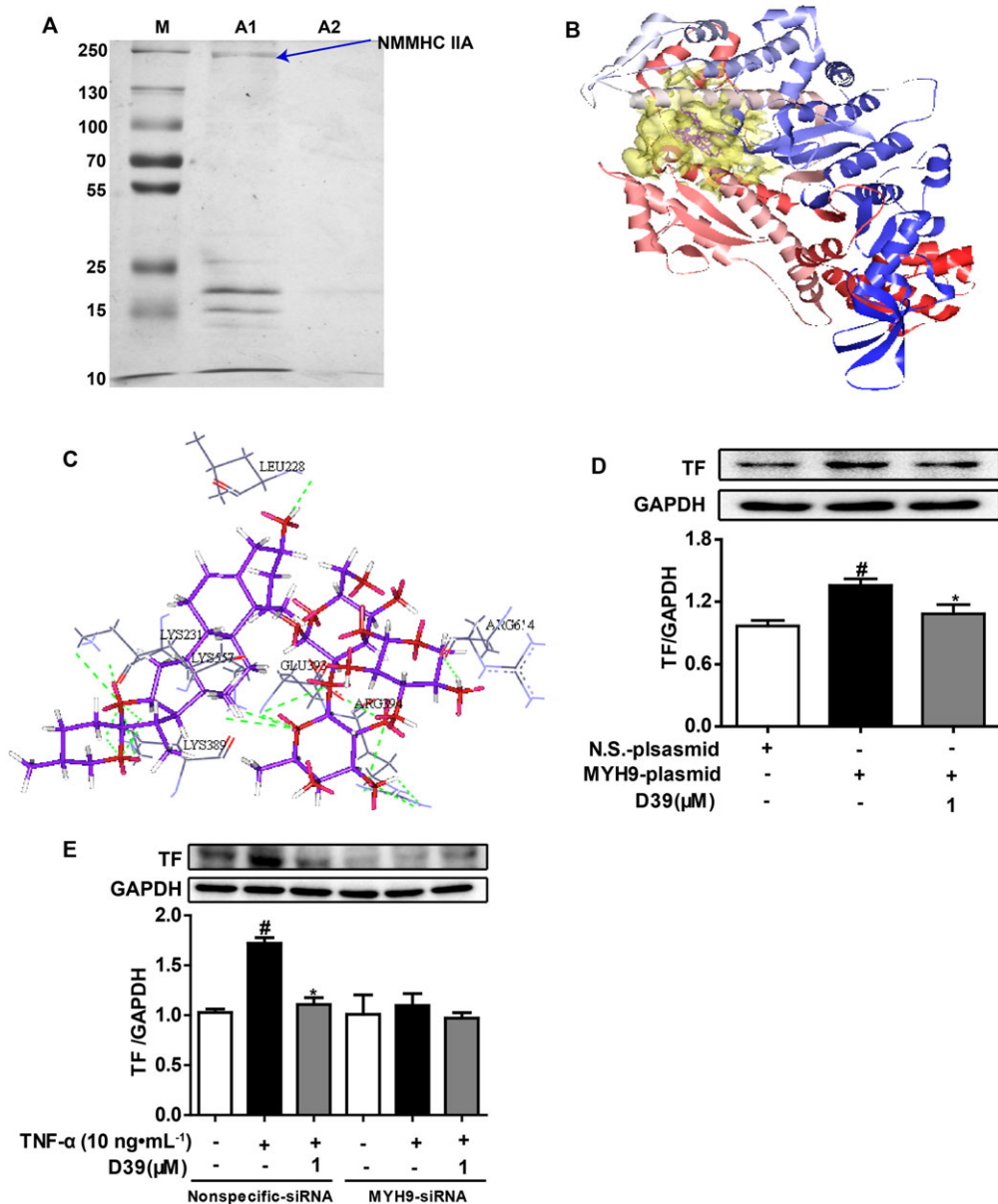
Figure 3

NMMHC IIA might be a key target protein involved in inhibition of TF expression by D39. (A) Covalent modifications of D39 on the affinity chromatography resin (Epoxy activated-sepharose 6B), which was used as a fixed-phase vector, were used to capture target proteins. NMMHC IIA was captured and identified as a D39-binding protein in endothelial cell lysates. (B) Molecular docking of D39 with a homology model of NMMHC IIA. The pocket was shown with the hydrophobic pocket rendered in transparent yellow, and D39 was shown in purple. (C) Amino acid residues within 5 Å, surrounding D39 in the pocket of NMMHC IIA. The H-bonding regions were rendered in dark red. (D) HEK 293T cells were transfected with an MYH9 plasmid or a control plasmid for 48 h. HEK 293T cells were pretreated with 1 μM D39 for 1 h and stimulated with TNF-α (10 ng·mL^{-1}) for 5 h. Total protein was analysed by Western blots. (E) HUVECs were transfected with 100 nM of MYH9-siRNA or control-siRNA for 48 h. HUVECs were pretreated with 1 μM D39 for 1 h and stimulated with TNF-α (10 ng·mL^{-1}) for 5 h. Total protein was analysed by Western blots. Data shown are the means ± SEM ($n = 5$ in five independent experiments) for the cell line experiments. $^{#}P < 0.05$, significantly different from the unstimulated group; $*P < 0.05$, significantly different from the TNF-α-stimulated group.

~230 kD protein, as indicated by SDS-PAGE, obviously decreased following serial affinity chromatography. MALDI-TOF-MS and Western blot analysis of the ~230 kD protein identified it as NMMHC IIA (Supporting Information Figure S2), suggesting that NMMHC IIA might be a specific binding protein of D39.

The docking study was carried out to explore the interaction of D39 with NMMHC IIA via GOLD 3.0.1. The docking results showed that 10 output conformers of the complex for D39 and NMMHC IIA had similar binding modes. The scaffold triterpene of D39 extended deep into the hydrophobic pocket of NMMHC IIA (Figure 3B), which interacted with

hydrophobic residues such as Leu[228], Lys[231], Lys[389], Glu[393], Arg[394], Lys[557] and Arg[614] (Figure 3C). Moreover, H-bonds formed between the hydroxyl at the C-12 position of the triterpene in D39 and Lys[231] as well as Lys[389], while the hydroxyls of the glycosides formed H-bonds with Leu[228], Lys[557], Glu[393], Arg[394] and Arg[614], which enhanced the binding affinity of D39 to NMMHC IIA.

To further corroborate the binding or interaction between D39 and NMMHC IIA, HEK293T cells were transiently transfected with human NMMHC IIA or empty vectors and were treated with D39. As shown in Figure 3D, NMMHC IIA overexpression in HEK293T cells significantly up-regulated TF expression. However, D39 (1 μM) markedly down-regulated TF expression in HEK293 cells that overexpressed NMMHC IIA. In addition, NMMHC IIA was successfully knocked down by an siRNA that specifically targeted MYH9 without affecting other myosin subtype expression in endothelial cells [data were shown in our previous report (Zhai *et al.,* 2015)]. NMMHC IIA knockdown significantly down-regulated TNF-α-induced TF protein expression (Figure 3E). Meanwhile, D39 significantly down-regulated TNF-α-induced TF protein expression in the negative-siRNA group but not in the MYH9-siRNA group.

D39 inhibited the disassociation of NMMHC IIA and TNFR2 in primary HUVECs

As previously documented (Zhai *et al.,* 2015), NMMHC IIA bound to TNFR2 and mediated signal internalization in TNF-α-stimulated endothelial cells. To investigate the inhibitory effect of D39 on NMMHC IIA in the regulation of TNFR2 signalling, we examined the potential protein–protein interaction (PPI) between NMMHCIIA and TNFR2 in untreated and TNF-α-stimulated primary HUVECs. As shown in Figure 4A, B, TNFR2 was co-localized and co-immunoprecipitated with NMMHCIIA in untreated cells, but not after TNF-α-stimulation. D39 inhibited the TNF-α-stimulated dissociation of NMMHC IIA from TNFR2. Similar results were obtained by the Duolink Proximity ligation assay (Figure 4C). These results suggest that TNF-α-stimulation disrupts the interaction between NMMHC IIA and TNFR2 and activates TNF-α-dependent signal internalization. Also D39 inhibits the TNF-α-stimulated dissociation of NMMHC IIA from TNFR2.

D39 inhibited venous thrombosis and plasma TF activity in vivo

To evaluate the effects of D39 on venous thrombus formation, the IVCL mouse model was utilized. The thrombus weight to length ratio was clearly increased in the IVCL mouse model compared with the sham group. Pretreatment with D39 reduced the thrombus weight to length ratio in a dose-dependent manner (Figure 5A, B). Meanwhile, H&E staining of the venous cross-section showed that the IVCL procedure led to dramatic thrombus formation after 48 h in mice treated with vehicle, as determined by the presence of a red thrombus (Figure 5D). In contrast, D39 administered at different doses significantly inhibited venous thrombosis. In addition, plasma was collected from the mouse eye socket as described previously (Zhai *et al.,* 2015). We further investigated the inhibitory effects of D39 on plasma TF procoagulant activity. A simplified chromogenic assay showed that D39 decreased plasma TF procoagulant activity in a dose-dependent manner (Figure 5C).

D39 suppressed endothelial TF expression by modulating GSK3β/p65 signalling pathways through inhibiting the dissociation of NMMHC IIA from TNFR2 in vivo

In the IVC-ligated mice, we assessed the effects of D39 on endothelial TF expression. As illustrated in Figure 6A, B, D39 (0.1–1 mg·kg^{-1}) inhibited endothelial TF expression in the IVCL group in a dose-dependent manner. Furthermore, we also investigated the effects of D39 on GSK3β and p65 activation. D39 significantly up-regulated phospho-GSK3β (Figure 6C) and down-regulated p65 expression (Figure 6D). Moreover, to confirm the interaction between NMMHC IIA and TNFR2 that was modulated by D39, we then examined whether D39 could inhibit the dissociation of NMMHC IIA from TNFR2 *in vivo*. As shown in Figure 6E, TNFR2 was co-localized with NMMHCIIA in sham-operated mice but not in IVC-ligated mice, and D39 inhibited the IVCL-induced dissociation of NMMHC IIA from TNFR2.

Discussion

The endothelium is one of the most important components in the pathogenesis of thrombotic and atherosclerotic disease (Ramot *et al.,* 2013). Endothelial cells also produce a variety of substances that regulate vessel tone, permeability, coagulation and fibrinolysis (Wakefield *et al.,* 2008). Adherence of cells and fibrin to intact endothelium is rarely seen. However, when the blood vessel wall is injured, the subendothelium is revealed. Platelets and other blood cells will immediately attach to the subendothelium, and the blood coagulation system becomes activated and forms clots (Mackman, 2012). In our previous study, we had demonstrated that the endothelial lining of blood vessels played a critical role in regulating thrombosis by preventing procoagulant and proinflammatory activities. NMMHC IIA in endothelial cells was a key upstream protein involved in TF expression and DVT. Inhibition or knockdown of endothelial NMMHC IIA decreased TF expression and thrombus formation, and this was mainly achieved through the Akt/GSK3β–NF-κB signalling pathway (Zhai *et al.,* 2015). However, there are not yet any natural antithrombotic products that target NMMHC IIA.

In this paper, based on molecular docking to NMMHC IIA and TF expression screening using 16 compounds from *L. muscari*, we identified a novel saponin D39 that down-regulated expression of TF, in low concentrations (1 μM) (Supporting Information Figure S1). This was also the first time that we had demonstrated the anti-thrombotic activity of D39 in IVC-ligated mice (Figure 5).

Our current study further demonstrated that NMMHC IIA was a potential target of D39, mediating its anti-thrombotic effects. D39 down-regulated TF expression and reduced DVT formation *in vitro* and *in vivo* through activation of the Akt/GSK3β signalling pathway and inhibition of the NF-κB signalling pathway (Figures 1, 2, 5 and 6), which was consistent with the results using the
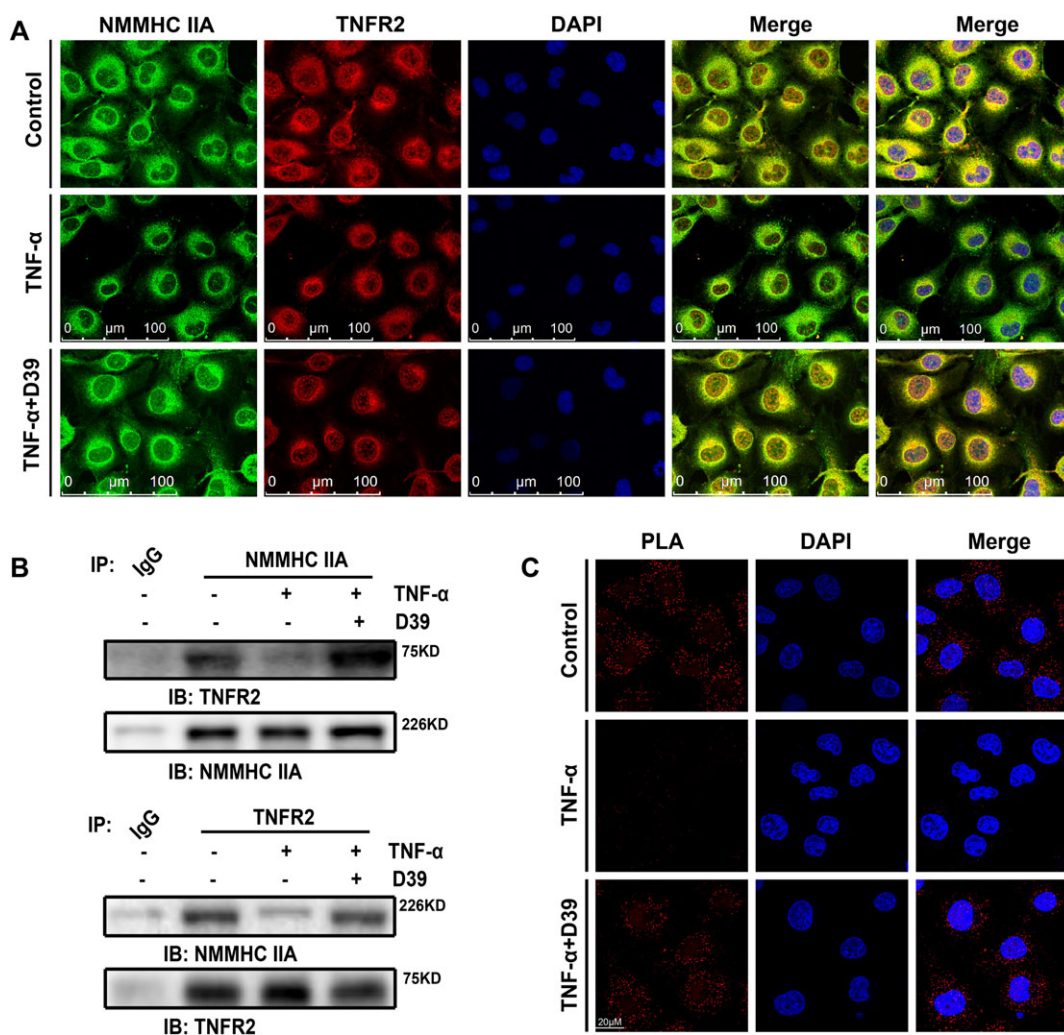
Figure 4

D39 inhibited the dissociation of NMMHC IIA from TNFR2. (A) Double-colour immunofluorescence analysis of NMMHC IIA (green) and TNFR2 (red) in primary HUVECs. Primary HUVECs were immunostained with a combination of anti-NMMHC IIA pAbs and anti-TNFR2 pAbs. Images were digitally merged. Representative results are shown. Scale bar, 100 μm. (B) Co-immunoprecipitation of NMMHC IIA and the TNFR2 from primary HUVEC lysates. Cells were harvested, lysed and immunoprecipitated with NMMHC IIA antibody or TNFR2 antibody. HUVEC lysate immunocomplexes were separated by SDS-PAGE and immunoblotted with the indicated antibodies. Normal serum (IgG) was used as a negative control for immunoprecipitation. (C) Confocal micrographs of primary HUVECs or D39-treated primary HUVECs (1 μM) in the presence or absence of 10 ng·mL^{-1} TNF-α for 8 min followed by the PLA reaction to show the NMMHC IIA–TNFR2 interaction (red signal) and DAPI (blue) staining. Scale bar, 20 μm. Representative images from five individual experiments with similar results are shown.

known NMMHC IIA inhibitor, blebbistatin (Zhai *et al.*, 2015). However, it was unclear whether the pharmacological effects of D39 were mediated through its effects on NMMHC IIA. NMMHC IIA overexpression up-regulated TF expression in HEK293T cells, which was significantly reversed by D39 (1 μM). NMMHC IIA knockdown down-regulated TNF-α-induced TF protein expression, while D39 did not affect TNF-α-induced TF protein expression in the MYH9-siRNA group (Figure 3). These findings indicated that the inhibitory activity of D39 on TF expression was dependent on NMMCH IIA. Furthermore, interactions between D39 and NMMHC IIA were assessed by serial affinity chromatography and molecular docking. Serial affinity chromatography is a classical pulldown method that has been applied to identify the targets of biologically

active compounds in cell or tissue lysates (Terstappen *et al.*, 2007; Ziegler *et al.*, 2013). The low MW ligand (probe) is immobilized on a solid phase and exposed to a protein extract (cell or tissue lysates) to bind the target protein(s). Subsequently, proteins that bind non-specifically to the probe and the matrix are removed by stringent washing prior to release of the bound proteins by eluting with a bioactive molecule or by heating. Finally, the target proteins are typically separated by SDS-PAGE and identified by immunodetection or mass spectrometry (Margarucci *et al.*, 2011; Margarucci *et al.*, 2013). Our results demonstrated that NMMHC IIA could be pulled down by D39 in cell lysates (Figure 3A and Supporting Information Figure S2). As previously documented, the myosin II holoenzyme consists of two molecules of
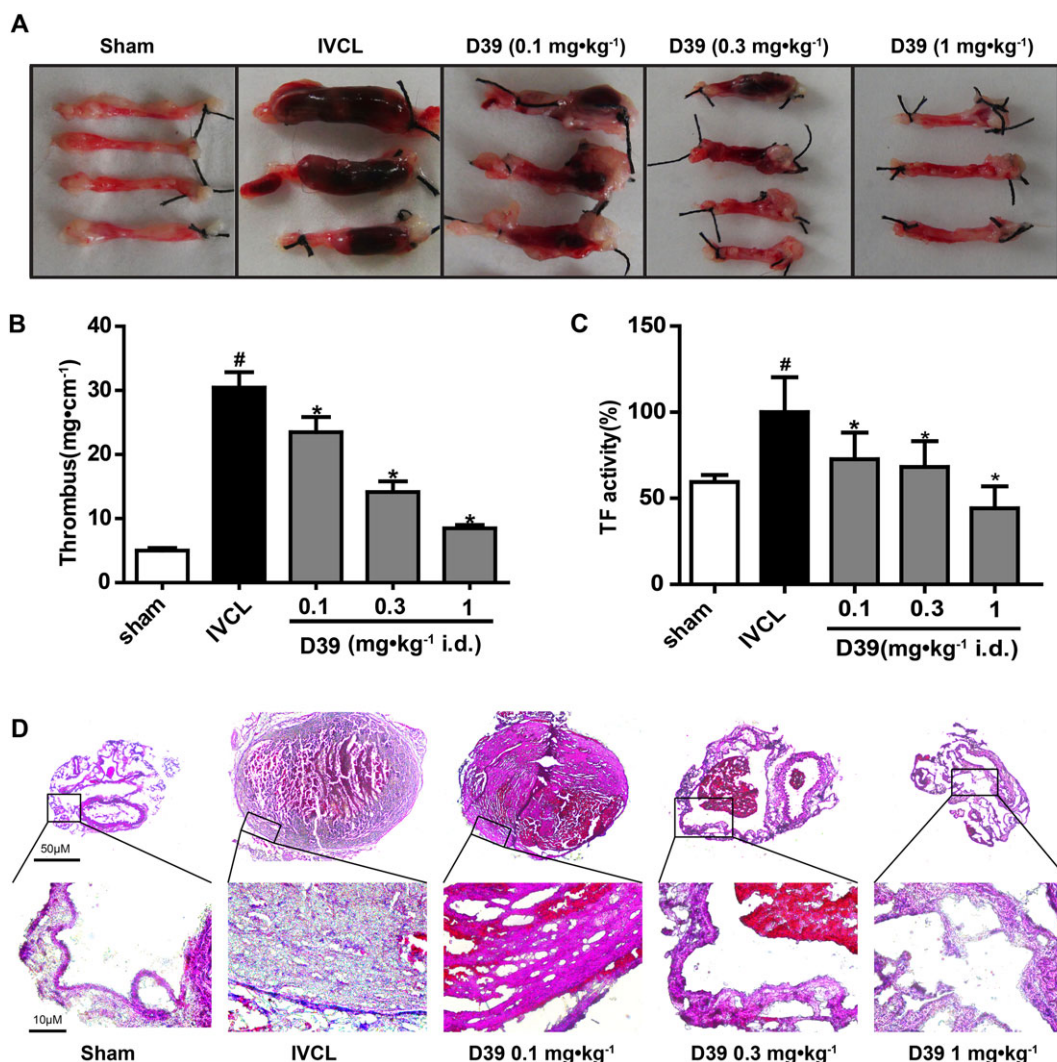
Figure 5

D39 inhibited venous thrombosis and plasma TF activity *in vivo*. mice were injected with vehicle (5% ethanol in saline) or D39 (0.1, 0.3 or 1 mg·kg^{-1}) i.p. and then the IVC was ligated to initiate thrombus formation, 1 h later. At 24 h after the surgical procedure, the mice were given D39 once, and plasma and IVCs were collected for further analysis at 48 h after the surgical procedure. (A, B) The IVC samples was weighed and the length of the thrombus was measured. The size of the thrombus was quantified as mg·cm^{-1} ($n = 8$). Three or more representative IVC from eight mice in each group as well as quantitative data ($n = 8$) of the IVC are shown. (C) TF procoagulant activity of plasma was examined with a chromogenic assay. (D) Histological evaluation of the ligated IVC. Histological analysis: representative photos of HE staining at 48 h after ligation (original magnification ×50 and ×400). Data shown are the means ± SEM of five mice per group. [#]$P < 0.05$, significantly different from the sham group; *$P < 0.05$, significantly different from the IVCL group.

myosin heavy chain (NMMHC II) and one molecule of the myosin regulatory light chain (MRLC, ~20 kDa) and the myosin essential light chain (MELC, ~17 kDa) associated with each NMMHC II at the neck region (Conti and Adelstein, 2008; Heissler and Manstein, 2013). Therefore, together with NMMHC IIA, low molecular weight MRLC and MELC (Figure 3A) should also be easily pulled down, which was confirmed in the previous report (Chandrasekharan *et al.*, 2013). In addition, molecular docking was used to accurately predict the structure of the ligand within the constraints of a receptor binding site and estimate the strength of binding (Yuriev and Ramsland, 2013). The docking results showed that all the parts of D39 extended deep into the hydrophobic pocket of NMMHC IIA

(Figure 3B) and formed H-bonds (Figure 3C), which further confirmed the binding affinity of D39 to NMMHC IIA.

Of note, PPIs play a key role in various biological processes (Zarzycka *et al.*, 2016). Similar to PPI inhibition, stabilization of dimers or oligomers can lead to either the activation or inhibition of a biological function. However, the stabilization of PPI complexes with low MW compounds (i.e. targeting regions at or near the interfaces of two or more proteins) can benefit from significantly higher specificity (Thiel *et al.*, 2012). Most of the low MW compounds that have been identified to modulate PPIs are inhibitors. Another promising way to interfere with PPI-associated biological processes is to promote PPI stabilization. Although PPI stabilizers are still scarce, stabilization of PPIs by low MW compounds is gaining
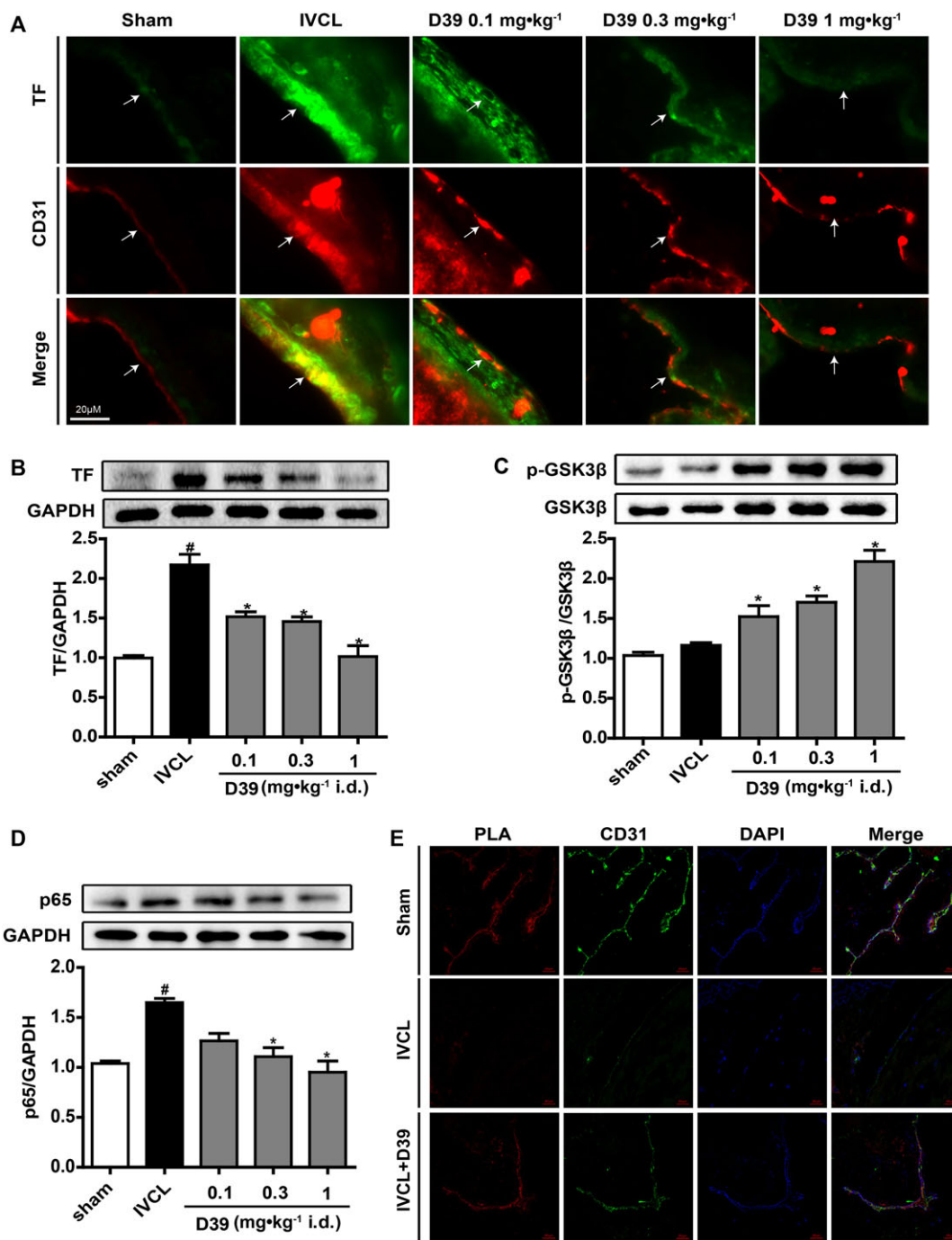
Figure 6

D39 suppressed endothelial TF expression by modulating the GSK3β/p65 signalling pathways through inhibiting the dissociation of NMMHC IIA from TNFR2 *in vivo*. (A) IVC frozen sections were prepared, and TF expression was analysed by immunofluorescence. (B) IVC lysates were prepared, and TF expression was analysed by Western blots. (C, D) IVC lysates were prepared, and p-GSK3β, GSK3β and p65 expressions were analysed by Western blots. (E) IVC frozen sections were prepared and used for PLA to confirm NMMHC IIA–TNFR2 interaction (red signal), CD31 staining (green) and DAPI staining (blue). Data shown are the means ± SEM of five mice per group. $^{\#}P < 0.05$, significantly different from the sham group; $^{*}P < 0.05$, significantly different from the IVCL group.

momentum and offers new pharmacological options (Zarzycka *et al.,* 2016). Our findings also demonstrated that D39 combined with NMMHC IIA to inhibit the dissociation of NMMHC IIA from TNFR2 (Figure 4), which was first reported using natural products. However, the particular

functional domains of NMMHC IIA that interact with D39 remain undefined. Blebbistatin is a powerful inhibitor of myosin IIA ATPase activity (Straight *et al.,* 2003; Kovacs *et al.,* 2004) but our findings demonstrated that D39 did not affect myosin II ATPase activity (data not shown), based on

a previous experiment (Chen *et al.,* 2016). It is possible that the functional domains of NMMHC IIA that interact with blebbistatin and D39 may be different. This possibility requires further investigation. Another saponin similar to D39, DT-13, exhibits no significant genotoxicity, acute toxicity or subchronic 90 day toxicity (Ma *et al.,* 2011), which suggest that D39 may have a comparable safety level. These results indicate that D39 is probably one of the most important candidate natural products for the prevention and treatment of DVT.

However, D39 is characterized by poor solubility and bioavailability (Gao *et al.,* 2012), which limits its pharmacological effects *in vivo*. In our experiments, D39 was delivered to mice, dissolved in 5% ethanol-saline, by i.p. injection. The dose of D39 *in vivo* was determined by a series of pilot experiments and a DT-13 preliminary study (Ma *et al.,* 2011). Furthermore, we tried to use aspirin or heparin sodium injection (1500 IU/kg) as a positive control (data not shown). The death rate of mice was clearly increased by i.p. injection of heparin sodium, due to severe postoperative bleeding. However, D39 or aspirin did not cause obvious bleeding. Previously, we found that the ethanol extract of Radix *O. japonicus* decreased the dried weight of venous thrombi, although with no effects on activated partial thromboplastin time, thrombin time and prothrombin time. These results indicated that D39 might inhibit thrombosis without affecting the anti-coagulation pathways (Kou *et al.,* 2005). The stability and pharmacokinetics of D39 *in vivo* will need to be addressed in further studies.

In the current study, we explored the effects of D39 on NMMHC IIA in the endothelial cells in terms of the pathogenesis of DVT *in vitro* and *in vivo*. However, NMMHC IIA is expressed not only in the endothelium (Chandrasekharan *et al.,* 2013) but also in monocytes/macrophages (Morrison *et al.,* 2014) and platelets (Leon *et al.,* 2007). Because of the complex pathological process of DVT, endothelium and other blood cells were key effector cells involved in DVT. Therefore, it is possible that D39 could also affect NMMHC IIA in monocytes/macrophages, and even neutrophils *in vivo*. This possibility is definitely worth further examination.

In summary, our findings uncovered a key role for D39 in inhibiting TF expression and activity through modulating NMMHC IIA–TNFR2 interaction and subsequently modulating the Akt/GSK3β–NF-κB signalling pathways (Figure 7). These results suggest that D39 might be useful in the clinical treatment of venous thrombosis and other inflammation-related vasculopathies. Our findings also provide a better understanding of the pharmacological activities of natural products, such as steroid saponins, on PPIs.

Acknowledgements

Author contributions

K.-F.Z., Y.-M.T., J.-R.Z., F.L. and Y.-Y. Z. carried out the laboratory experiments, collected and analysed the data and interpreted the results. K.-F.Z. and Y.-N.L. performed molecular docking analysis. K.-F.Z., and J.-P.K. designed the experiments and wrote the manuscript. J.Q. provided the tested compounds. Z.G. analysed the data and revised the manuscript. J.-P.K. and B.-Y.Y. designed the experiments, supervised the study and revised the manuscript.

Conflict of interest

The authors declare no conflicts of interest.

Declaration of transparency and scientific rigour

This Declaration acknowledges that this paper adheres to the principles for transparent reporting and scientific rigour of preclinical research recommended by funding agencies, publishers and other organisations engaged with supporting research.
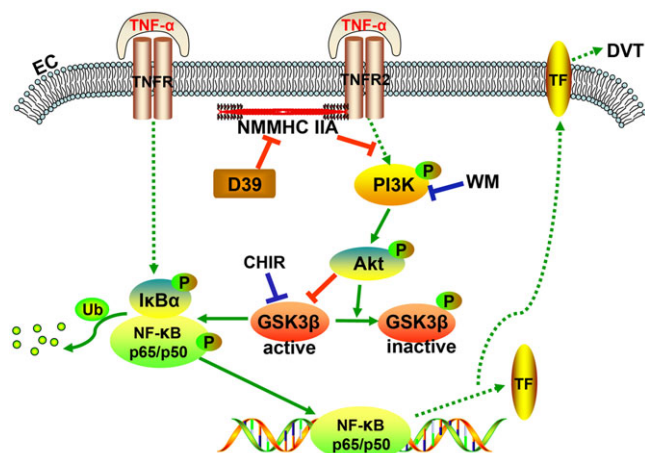

Figure 7

Diagram showing the pathways that mediate the inhibition of TF expression in endothelial cells *in vitro* and CD31-positive cells *in vivo* by D39 following inflammatory stimulation and IVCL.

References

Alexander SPH, Fabbro D, Kelly E, Marrion N, Peters JA, Benson HE *et al.* (2015a). The Concise Guide to PHARMACOLOGY 2015/16: Catalytic receptors. Br J Pharmacol 172: 5979–6023.

Alexander SPH, Fabbro D, Kelly E, Marrion N, Peters JA, Benson HE *et al.* (2015b). The Concise Guide to PHARMACOLOGY 2015/16: Enzymes. Br J Pharmacol 172: 6024–6109.

Alexander SPH, Kelly E, Marrion N, Peters JA, Benson HE, Faccenda E *et al.* (2015c). The Concise Guide to PHARMACOLOGY 2015/16: Overview. Br J Pharmacol 172: 5734–5143.

Badirou I, Pan J, Souquere S, Legrand C, Pierron G, Wang A *et al.* (2015). Distinct localizations and roles of non-muscle myosin II during proplatelet formation and platelet release. J Thromb Haemost 13: 851–859.

Banerji S, Wright AJ, Noble M, Mahoney DJ, Campbell ID, Day AJ *et al.* (2007). Structures of the Cd44-hyaluronan complex provide insight into a fundamental carbohydrate-protein interaction. Nat Struct Mol Biol 14: 234–239.

Calaminus SD, Auger JM, McCarty OJ, Wakelam MJ, Machesky LM, Watson SP (2007). MyosinIIa contractility is required for maintenance of platelet structure during spreading on collagen and contributes to thrombus stability. J Thromb Haemost 5: 2136–2145.

Chandrasekharan UM, Dechert L, Davidson UI, Waitkus M, Mavrakis L, Lyons K *et al.* (2013). Release of nonmuscle myosin II from the cytosolic domain of tumor necrosis factor receptor 2 is required for target gene expression. Sci Signal 6: ra60.

Chen HL, Zhao J, Zhang GJ, Kou JP, Yu BY (2016). An optimized micro-assay of myosin II ATPase activity based on the molybdenum blue method and its application in screening natural product inhibitors. Chin J Nat Med 14: 421–426.

Conti MA, Adelstein RS (2008). Nonmuscle myosin II moves in new directions. J Cell Sci 121: 11–18.

Curtis MJ, Bond RA, Spina D, Ahluwalia A, Alexander SP, Giembycz MA *et al.* (2015). Experimental design and analysis and their reporting: new guidance for publication in BJP. Br J Pharmacol 172: 3461–3471.

Gao S, Basu S, Yang Z, Deb A, Hu M (2012). Bioavailability challenges associated with development of saponins as therapeutic and chemopreventive agents. Curr Drug Targets 13: 1885–1899.

Guha M, Mackman N (2002). The phosphatidylinositol 3-kinase-Akt pathway limits lipopolysaccharide activation of signaling pathways and expression of inflammatory mediators in human monocytic cells. J Biol Chem 277: 32124–32132.

Heissler SM, Manstein DJ (2013). Nonmuscle myosin-2: mix and match. Cell Mol Life Sci 70: 1–21.

Huang YL, Kou JP, Ma L, Song JX, Yu BY (2008). Possible mechanism of the anti-inflammatory activity of ruscogenin: role of intercellular adhesion molecule-1 and nuclear factor-kappaB. J Pharmacol Sci 108: 198–205.

Ju J, Qi Z, Cai X, Cao P, Huang Y, Wang S *et al.* (2012). The apoptotic effects of toosendanin are partially mediated by activation of deoxycytidine kinase in HL-60 cells. PloS one 7: e52536.

Kilkenny C, Browne W, Cuthill IC, Emerson M, Altman DG (2010). Animal research: reporting in vivo experiments: the ARRIVE guidelines. Br J Pharmacol 160: 1577–1579.

Kou J, Tian Y, Tang Y, Yan J, Yu B (2006). Antithrombotic activities of aqueous extract from Radix *Ophiopogon japonicus* and its two constituents. Biol Pharm Bull 29: 1267–1270.

Kou J, Yu B, Xu Q (2005). Inhibitory effects of ethanol extract from Radix *Ophiopogon japonicus* on venous thrombosis linked with its endothelium-protective and anti-adhesive activities. Vascul Pharmacol 43: 157–163.

Kovacs M, Toth J, Hetenyi C, Malnasi-Csizmadia A, Sellers JR (2004). Mechanism of blebbistatin inhibition of myosin II. J Biol Chem 279: 35557–35563.

Leon C, Eckly A, Hechler B, Aleil B, Freund M, Ravanat C *et al.* (2007). Megakaryocyte-restricted MYH9 inactivation dramatically affects hemostasis while preserving platelet aggregation and secretion. Blood 110: 3183–3191.

Li YD, Ye BQ, Zheng SX, Wang JT, Wang JG, Chen M *et al.* (2009). NF-kappaB transcription factor p50 critically regulates tissue factor in deep vein thrombosis. J Biol Chem 284: 4473–4483.

Liu J, Chen T, Yu B, Xu Q (2002). Ruscogenin glycoside (Lm-3) isolated from *Liriope muscari* inhibits lymphocyte adhesion to extracellular matrix. J Pharm Pharmacol 54: 959–965.

Liu Z, van Grunsven LA, Van Rossen E, Schroyen B, Timmermans JP, Geerts A *et al.* (2010). Blebbistatin inhibits contraction and accelerates migration in mouse hepatic stellate cells. Br J Pharmacol 159: 304–315.

Lv Y, Lu S, Lu T, Kou J, Yu B (2013). Homology model of nonmuscle myosin heavy chain IIA and binding mode analysis with its inhibitor blebbistatin. J Mol Model 19: 1801–1810.

Ma S, Kou J, Yu B (2011). Safety evaluation of steroidal saponin DT-13 isolated from the tuber of *Liriope muscari* (Decne.) Baily. Food Chem Toxicol 49: 2243–2251.

Mackman N (2008). Triggers, targets and treatments for thrombosis. Nature 451: 914–918.

Mackman N (2012). New insights into the mechanisms of venous thrombosis. J Clin Invest 122: 2331–2336.

Maravillas-Montero JL, Santos-Argumedo L (2012). The myosin family: unconventional roles of actin-dependent molecular motors in immune cells. J Leukoc Biol 91: 35–46.

Margarucci L, Monti MC, Cassiano C, Mozzicafreddo M, Angeletti M, Riccio R *et al.* (2013). Chemical proteomics-driven discovery of oleocanthal as an Hsp90 inhibitor. Chem Commun 49: 5844–5846.

Margarucci L, Monti MC, Fontanella B, Riccio R, Casapullo A (2011). Chemical proteomics reveals bolinaquinone as a clathrin-mediated endocytosis inhibitor. Mol Biosyst 7: 480–485.

McGrath JC, Lilley E (2015). Implementing guidelines on reporting research using animals (ARRIVE etc.): new requirements for publication in BJP. Br J Pharmacol 172: 3189–3193.

Morrison AR, Yarovinsky TO, Young BD, Moraes F, Ross TD, Ceneri N *et al.* (2014). Chemokine-coupled beta2 integrin-induced macrophage Rac2-Myosin IIA interaction regulates VEGF-A mRNA stability and arteriogenesis. J Exp Med 211: 1957–1968.

Ono A, Westein E, Hsiao S, Nesbitt WS, Hamilton JR, Schoenwaelder SM *et al.* (2008). Identification of a fibrin-independent platelet contractile mechanism regulating primary hemostasis and thrombus growth. Blood 112: 90–99.

Ramot Y, Nyska A, Spectre G (2013). Drug-induced thrombosis: an update. Drug Saf 36: 585–603.

Schulz C, Engelmann B, Massberg S (2013). Crossroads of coagulation and innate immunity: the case of deep vein thrombosis. J Thromb Haemost Suppl 1: 233–241.

Singh I, Smith A, Vanzieleghem B, Collen D, Burnand K, Saint-Remy JM *et al.* (2002). Antithrombotic effects of controlled inhibition of factor VIII with a partially inhibitory human monoclonal antibody in a murine vena cava thrombosis model. Blood 99: 3235–3240.

Soderberg O, Leuchowius KJ, Gullberg M, Jarvius M, Weibrecht I, Larsson LG *et al.* (2008). Characterizing proteins and their

interactions in cells and tissues using the in situ proximity ligation assay. Methods 45: 227–232.

Southan C, Sharman JL, Benson HE, Faccenda E, Pawson AJ, Alexander SP *et al.* (2016). The IUPHAR/BPS Guide to PHARMACOLOGY in 2016: towards curated quantitative interactions between 1300 protein targets and 6000 ligands. Nucleic Acids Res 44: D1054–D1068.

Straight AF, Cheung A, Limouze J, Chen I, Westwood NJ, Sellers JR *et al.* (2003). Dissecting temporal and spatial control of cytokinesis with a myosin II Inhibitor. Science 299: 1743–1747.

Sun L, Lin S, Zhao R, Yu B, Yuan S, Zhang L (2010). The saponin monomer of dwarf lilyturf tuber, DT-13, reduces human breast cancer cell adhesion and migration during hypoxia via regulation of tissue factor. Biol Pharm Bull 33: 1192–1198.

Sun Q, Chen L, Gao M, Jiang W, Shao F, Li J *et al.* (2012). Ruscogenin inhibits lipopolysaccharide-induced acute lung injury in mice: involvement of tissue factor, inducible NO synthase and nuclear factor (NF)-kappaB. Int Immunopharmacol 12: 88–93.

Terstappen GC, Schlupen C, Raggiaschi R, Gaviraghi G (2007). Target deconvolution strategies in drug discovery. Nat Rev Drug Discov 6: 891–903.

Thiel P, Kaiser M, Ottmann C (2012). Small-molecule stabilization of protein-protein interactions: an underestimated concept in drug discovery? Angew Chem Int Ed Engl 51: 2012–2018.

Tian Y, Ma S, Lin B, Kou J, Yu B (2013). Anti-thrombotic activity of DT-13, a saponin isolated from the root tuber of *Liriope muscari*. Indian J Pharmacol 45: 283–285.

Trott O, Olson AJ (2010). AutoDock Vina: improving the speed and accuracy of docking with a new scoring function, efficient optimization, and multithreading. J Comput Chem 31: 455–461.

Wakefield TW, Myers DD, Henke PK (2008). Mechanisms of venous thrombosis and resolution. Arterioscler Thromb Vasc Biol 28: 387–391.

Yamamoto K, Yamazaki A, Takeuchi M, Tanaka A (2006). A versatile method of identifying specific binding proteins on affinity resins. Anal Biochem 352: 15–23.

Yuriev E, Ramsland PA (2013). Latest developments in molecular docking: 2010–2011 in review. J Mol Recognit 26: 215–239.

Zarzycka B, Kuenemann MA, Miteva MA, Nicolaes GA, Vriend G, Sperandio O (2016). Stabilization of protein-protein interaction complexes through small molecules. Drug Discov Today 21: 48–57.

Zhai K, Tang Y, Zhang Y, Li F, Wang Y, Cao Z *et al.* (2015). NMMHC IIA inhibition impedes tissue factor expression and venous thrombosis via Akt/GSK3beta-NF-kappaB signalling pathways in the endothelium. Thromb Haemost 114: 173–185.

Zhang W, Wang J, Wang H, Tang R, Belcher JD, Viollet B *et al.* (2010). Acadesine inhibits tissue factor induction and thrombus formation by activating the phosphoinositide 3-kinase/Akt signaling pathway. Arterioscler Thromb Vasc Biol 30: 1000–1006.

Ziegler S, Pries V, Hedberg C, Waldmann H (2013). Target identification for small bioactive molecules: finding the needle in the haystack. Angew Chem Int Ed Engl 52: 2744–2792.

Supporting Information

Figure S1 Effects of saponins from *L. muscari* on docking energy and TNF-α-induced TF expression. (A) Docking energies of saponin compounds bound to NMMHC IIA via GOLD 3.0.1. (B) Saponins showed different inhibitory effects on TF expression. All of the saponins were used at the concentration of 1 μM. Data shown are the means ± SEM (n = 5 in five individual experiments) for the cell line experiments. #P < 0.05, significantly different from the unstimulated group; *P < 0.05, significantly different from the TNF-α-stimulated group.

Figure S2 Capture and identification of NMMHC IIA as a D39-binding protein. (A) Amino acid sequence of human NMMHC IIA. The amino acid residues in human NMMHC IIA indicate the peptides detected by tryptic digestion and MS analyses. (B) Confirmation of the 230-kD protein using an NMMHC IIA-specific antibody.

Figure S3 D39 activated the PI3K/Akt signalling pathway and inhibited TF expression in TNF-α-induced endothelial cells. (A) TF expression in endothelial cells was examined by Western blot at 5 h after treatment with TNF-α (10 ng mL^{-1}), TNF-α and D39 (1 μM) or TNF-α and D39 with CHIR99021 (5 μM). (B) TF expression in endothelial cells was examined by Western blot at 5 h after treatment with TNF-α (10 ng mL^{-1}), TNF-α and D39 (1 μM) or TNF-α and D39 with wortmannin (10 μM). Data shown are the means ± SEM (n = 5 in five individual experiments) for the cell line experiments. #P < 0.05, significantly different from the unstimulated group; *P < 0.05, significantly different from the TNF-α-stimulated group.